Applied Water Science (2019) 9:108
https://doi.org/10.1007/s13201-019-0979-8

ORIGINAL ARTICLE

Lead ion removal from water by hydroxyapatite nanostructures synthesized from egg sells with microwave irradiation

Fatemeh Safatian[1] · Zahra Doago[2] · Marzieh Torabbeigi[3] · Hossein Rahmani Shams[2] · Nastaran Ahadi[4]

Received: 25 February 2019 / Accepted: 12 May 2019 / Published online: 24 May 2019

Abstract
Hydroxyapatite nanostructures were synthesized by microwave irradiation from egg shells. This nanoadsorbent was used for effective removal of lead ions from water and wastewater samples. The effects of experimental conditions such as pH, temperature, contact time, dose of adsorbent and initial concentration of lead ions on removal were investigated. Langmuir and Freundlich isotherms were studied, and the results indicated that the adsorption mechanism was based on Langmuir isotherm. The synthesized nanoadsorbent shows high adsorption capacities for removal of lead ion from water samples.

Keywords Hydroxyapatite · Nanoparticles · Adsorption · Langmuir · Freundlich · Lead

Introduction

Widespread use of lead in various industries such as battery manufacturing, radiation shielding, acid metal plating, ammunition, tetraethyl lead manufacturing, ceramic and glass industries printing, painting, water piping and other industries can release lead into environment (Mager et al. 2011). Lead can cause negative effects on the environment when it accumulates in living systems. Lead poisoning causes damage to the human biological systems such as nervous system, liver, kidney, brain and reproductive system (Fergusson 1990).

Several different processes have been developed for removal of heavy metals from aqueous media such as electrodialysis, chemical precipitation, adsorption, solvent extraction, reverse osmosis, ultrafiltration or ion exchange (Gritlin 1988; Davis and Comwell 1991). Adsorption process has been shown good effectiveness, efficiency, economically feasibility to remove heavy metal such as application of waste biomass (Cheng et al. 2016), modified ligno-cellulosic material (Huang et al. 2015) and wheat straw (Wu et al. 2019). Many different adsorbents such as natural zeolite (Faghihian et al. 1999; Pansini and Collella 1990), aquatic plant (Srivastav et al. 1993), fly ash sub grades (Laumakis et al. 1995), ion exchange resin (Hewitt et al. 1991), activated carbon (Reed et al. 1994; Gupta et al. 1997) have been used for lead removal from aquatic samples.

Synthesis and application of nanocompounds for various purposes have been considered such as the application of mesoporous compounds as catalyst (Malgras et al. 2016, 2018), synthesis of nanocrystals with special optical and electronic properties (Li et al. 2014; Tan et al. 2017), the use of nanoparticles as adsorbent for water and wastewater treatment (Hamidzadeh et al. 2015). Various nanomaterials were developed to removal heavy metals from aqua samples. The physical and chemical properties of nanomaterials have led to enhance the removal efficiency (Lu and Astruc 2018).

Hydroxyapatite (HA) is a class of calcium phosphate-based bioceramics with chemical composition of $Ca_{10}(PO_4)_6(OH)_2$. HA is used for different applications such as drug delivery (Pon-On et al. 2011; Zhang et al. 2010), coating implants (Kold et al. 2006) and other biomedical areas (Chen et al. 2011a, b). It is also an ideal material for removing heavy metals. The morphology and structure of HA are strongly affected by the method of preparation. Various different methods have been developed for synthesis of hollow spheres HA such as microwave-assisted

✉ Marzieh Torabbeigi
torabbeigi@gmail.com

[1] Ramsar International Branch, Mazandaran University of Medical Sciences, Ramsar, Iran

[2] Department of Chemistry, Varamin Branch, Payam Noor University, Tehran, Iran

[3] School of Pablic Health and Safety, Shahid Beheshti University of Medical Sciences, Tehran, Iran

[4] Pharmaceutical Science Branch, Islamic Azad University, Tehran, Iran

hydrothermal routes (Wang et al. 2011), DNA-template hydrothermal methods (Qi et al. 2012), ion-assisted mineralization methods (Jiang et al. 2012), and others.

The egg shells contain natural organic and inorganic compounds, while a large amount of them is discarded as biowaste every day. To recycle them, this biowaste can be used to make effective adsorbents to remove toxins from the water. In the present work, the flower liked HA, which synthesized from egg shells by microwave oven, was used for lead ion removal from water samples.

Methods and materials

Ethylene diamine tetra acetic acid (EDTA), sodium hydroxide, sodium dihydrogen phosphate and sodium hypochlorite were prepared from Merck, Germany. Lead stock solution (1000 mg L^{-1}) was purchased from Merck, Germany. Double distilled water was used for all experiments.

For preparation of nanoadsorbent, the egg shells were collected from household consumption for a week. The egg shells were placed in boiling water for 30 min and then washed to remove inner membranes with cold water. They were placed in a sodium hypochlorite solution (1 M) for 2 days. They were washed and dried at 110 °C for 5 h and then powdered.

500 ml EDTA 0.1 M was added to 5 g egg shells powder and stirred for 2 h until all carbon dioxide was removed from solution. Then, 2.50 ml Na_2HPO_4 0.6 M was slowly added to breaker for 30 min and then pH of solution was adjusted to 13 by sodium hydroxide solution. The solution was put in microwave with 680 W powers for 30 min. The resulted precipitate was filtered and washed with water tree times and dried at 110 °C for 5 h (Kumar and Girija 2013).

The scanning electron microscopy (SEM) image of synthesized nanostructure (Fig. 1) was obtained by the SEM (TSCAN, Check). As shown in Fig. 1, the flowerlike HA nanostructure formed leafs with width less than 100 nm and length about 500 nm which are extending radially from center.

FT-IR spectrum of nanostructure (Fig. 2) showed in 450–4000 cm^{-1} resolution was obtained by PerkinElmer (USA) spectrum 2 with KBr pellet technique at temperature room. FT-IR spectrum was recorded in 3 regions (ν_1) 873.5 cm^{-1} (ν_2) 1416.4 cm^{-1}, and (ν_3) 1458.3 cm^{-1} which represents formation of hydroxyl apatite.

In discontinuous method, lead solution 100 mg L^{-1} was prepared from stock solution (1 g L^{-1}). 10 ml of 100 mg L^{-1} solution was transferred into 50-ml breaker, and then 0.01 g of nanoadsorbent was added, stirred for 1 h and centrifuged. Lead concentration was determined with atomic absorption technique (Varian 200).

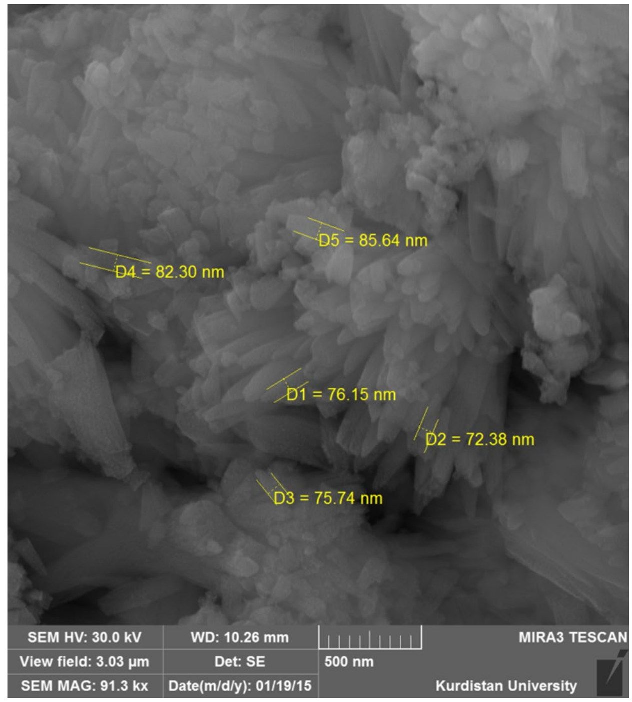

Fig. 1 SEM image of synthesized HA with microwave

Elimination efficiency of lead ion was improved by investigation of effective parameters such as contact time, initial concentration, pH solution and dose of nanoadsorbent.

The lead adsorption into the nano-HA was calculated by following equation

$$q_e = \left(c_0 - c_e\right)\frac{v}{w}$$

Where q_e is the dose of adsorbed metal per grams of Nano HA (mgg^{-1}), v is volume of solution (L), w is the weight of adsorbent (g), and the C_0 and C_e are the initial and equilibrium concentration of metal in solution (mgL^{-1}), respectively.

Results and discussion

In the present study, adsorption process was used as refining technology to remove lead ions from water and wastewater samples by nanostructure adsorbent. Elimination efficiency of lead ion was improved by investigation of effective parameters such as temperature, contact time, initial concentration and pH solution.

To investigate the effect of pH on removal process, 15 ml of 20 mg L^{-1} of lead solution was exposed to 0.01 g nano HA at 24 ± 1 °C with 500 rpm stirred rate for an hour. The pH value was varied from 3 to 9 by addition of 1 $molL^{-1}$ hydrochloric acid or sodium hydroxide solutions. pH is the

Fig. 2 FT-IR spectrum of synthesized HA

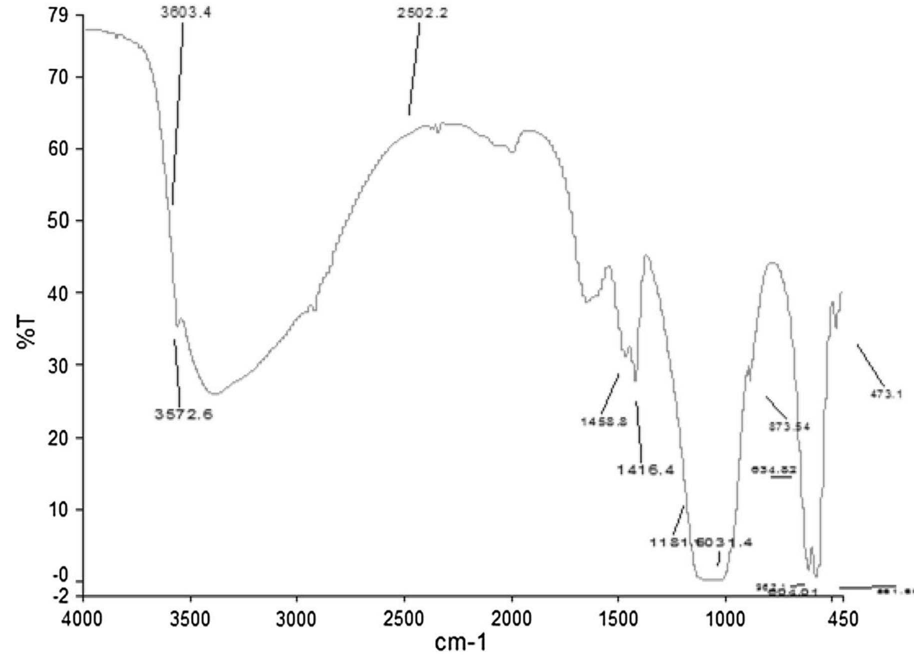

effective parameters in removing process of heavy metal ions from wastewater samples. As shown in Fig. 3a, the percentages of lead ion removal at different pH were shown that maximum removal was occurred in pH = 7, whereas this pH is optimal pH and would be used for other experiments.

The contact time is one of the most effective factors in the adsorption process. To investigate the effect of contact time on adsorption, the experiments were done in different contact times from 5 to 60 min with 20 mg L^{-1} initial concentration of lead ions and 0.01 g nanoparticles weight at pH = 7 and 24 ± 1 °C temperature. Figure 3b shows that the rate of adsorption in the early stages is rapid and gradually decreases over time and after reaching the equilibrium state, it remains almost constant. The adsorption of lead ions was reached to equilibrium state after 15 min with 99.8% removal.

The adsorption of lead ions raised by increasing dose of adsorbent due to increase adsorption sites. The amounts of adsorption were increased by increasing the dose of nanoparticle from 0.001 to 0.05 g (Fig. 3c).

Adsorption isotherms are intended to describe adsorption capacity in order to facilitate the evaluation of this process. Among the various types of available isotherms, Langmuir and Freundlich isotherms, which are commonly used

Fig. 3 The effects of **a** pH, **b** contact time and **c** dose of adsorbent on removal of lead ion by HA nanoparticles

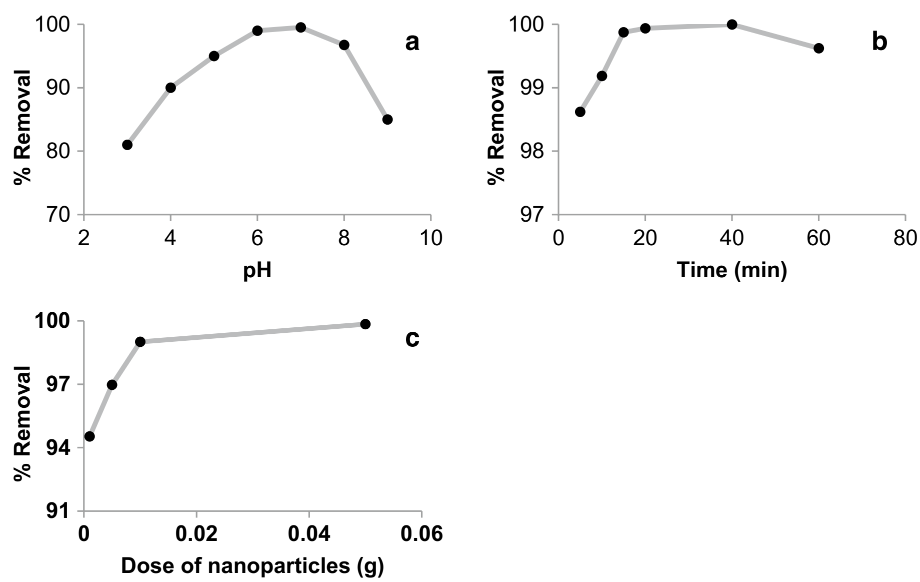

for adsorption modeling, are studied. In this study, 100 ml of lead solution at concentrations of 15–1000 mg L^{-1} was contacted for 15 min with 10 mg of nanoparticles at pH 7, 500 rpm and 24 °C, and then it was filtered with a filter paper and vacuum pump. Finally, the concentration of the remaining ions was read by the atomic adsorption device, the amount of adsorbed ions was measured, and the lead adsorption isotherms were plotted. The fitting of Langmuir and Freundlich adsorption models was studied, and its results were investigated for isotherms adsorption and modeling.

Used Langmuir equation for equilibrium adsorption is:

$$\frac{c_e}{q_e} = \frac{1}{Q_0 \times b} + \frac{c_e}{Q_0}$$

Where C_e is equilibrium concentration of metal in solution (mgL^{-1}), q_e is the dose of adsorbed metal per unit weight adsorption (mgg^{-1}), Q_0 and b are Langmuir constants that related to the adsorbent capacity and adsorbent energy. Ce/qe versus Ce is plotted in Fig. 4a, and the Langmuir constant is tabulated in Table 1.

Adsorption process was modeled with Freundlich isotherm with following equation

$$q_e = k_f c_e^{\frac{1}{n}}$$

where C_e is the equilibrium concentration of metal in solution (mg L^{-1}), q_e is the dose of adsorbed metal (mg g^{-1}), k_f and n are Freundlich adsorption constants. The Logarithmic equation of Freundlich model can be writhen as:

$$\log q_e = \log k_f + \frac{1}{n} \log c_e$$

By plotted Log q_e versus log C_e, the straight line was resulted that the slop and intercept of line represented n^{-1} and log k_f, respectively. Figure 4b shows the Logarithmic plot of Freundlich model, and the Freundlich adsorption constants is tabulated in Table 1. The obtained result in Table 1 showed that adsorption process had compatibility with Langmuir isotherm.

In this research, the nanostructure hydroxyapatite adsorbent was synthesized from eggshell and used to eliminate lead ion from water samples. The results showed that the removal procedure was done with low adsorption energy

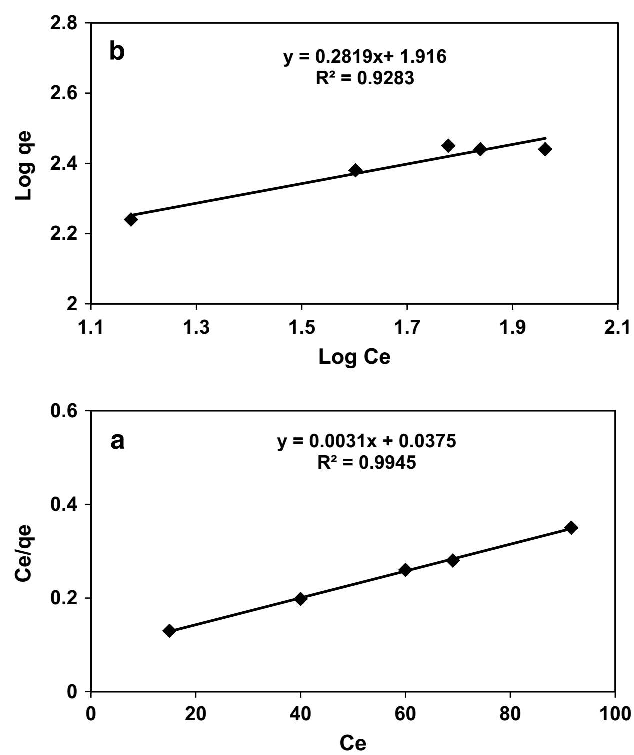

Fig. 4 **a** Langmuir and **b** Freundlich isotherms

Table 1 Langmuir and Freundlich constants of absorption isotherms curves

Freundlich			Langmuir		
k_f	n	Correlation constant	Q_0	b	Correlation constant
6.82	3.54	0.928	322.6	0.083	0.994

Table 2 Comparative values of maximum adsorption capacity (Q_m) of some adsorbent to remove lead ion from water which reported in 2018 publications

Adsorbant	Q_m (mg g^{-1})
Ternary layered double hydroxide (Co–Zn–Al LDH) intercalated with carbonate	130.3 (Abasi et al. 2018)
Chelating polyacrylonitrile beads	145 (Bhunia et al. 2018)
Tomato waste	152 (Heraldy et al. 2018)
Oxidized mesoporous carbon	198.6 (Zhang et al. 2018)
Silicated orange peel waste nanocomposites	200 (Saini et al., 2018)
Magnetic biochar	206.5 (Chen et al. 2018)
Steel-making dust	208.9 (Bouabidi et al. 2018)
Modified walnut shell	221.2 (Li et al. 2018a)
Silica nanofiber/magnetite nanoparticles/porous silica	243.9 (Li et al. 2018b)
1,8-dihydroxyanthraquinone (DHAQ) functionalized graphene oxide	283.5 (Khazaei et al. 2018)
Hroxyappatite Nanostructures Synthesized from Eggshell	322.6 (Present work)
TiO_2@C nanosheets	331.7 (Gan et al. 2019)
MoS_2/CeO_2 nanohybrids	333 (Tong et al. 2018)
$Fe_3O_4/Sr_5(PO_4)_3(OH)$	401(Zhang et al. 2019)
Hydroxyapatite/alginate/gelatin nanocomposites	616 (Sangeetha et al. 2018)
Zeolite-imidazolate framework	1348 (Huang et al. 2018)

(8.3×10^{-2} L mg^{-1}) and high (322.6 mg g^{-1}). The adsorption capacity was measured after 2 months, and no significant difference was observed. Table 2 shows the maximum adsorption capacity of some adsorbent to remove lead ion which published in 2018 papers. Although, some of the maximum adsorption capacities, reported in Table 2, are greater than those obtained in this study, the effective nanostructure hydroxyapatite adsorbent has been synthesized from recycled biowaste by a simple and inexpensive method.

Compliance with ethical standards

Conflict of interest The authors declare that they have no conflict of interest.

References

Abasi CY, Diagboya PNE, Dikio ED (2018) Layered double hydroxide of cobalt–zinc–aluminium intercalated with carbonate ion: preparation and Pb(II) ion removal capacity. Int J Environ Stud 76:251–265

Bhunia P, Chatterjee S, Rudra P, De S (2018) Chelating polyacrylonitrile beads for removal of lead and cadmium from wastewater. Sep Purif Technol 193:202–213

Bouabidi ZB, El-Naas MH, Cortes D, McKay G (2018) Steel-making dust as a potential adsorbent for the removal of lead(II) from an aqueous solution. Chem Eng J 334:837–844

Chen F, Huang P, Zhu YJ, Wu J, Zhang CL, Cui DX (2011a) The photoluminescence, drug delivery and imaging properties of multifunctional Eu3+/Gd3+ dual-doped hydroxyapatite nanorods. Biomaterials 32:9031–9039

Chen F, Zhu YJ, Zhang KH, Wu J, Wang KW, Tang QL, Mo XM (2011b) Europium-doped amorphous calcium phosphate porous nanospheres: preparation and application as luminescent drug carriers. Nanoscale Res Lett 6:67

Chen YD, Ho SH, Wang D, Wei ZS, Chang JS, Ren NQ (2018) Lead removal by a magnetic biochar derived from persulfate-ZVI treated sludge together with one-pot pyrolysis. Biores Technol 247:463–470

Cheng Y, Yang C, He H, Zeng G, Zhao K, Yan Z (2016) Biosorption of Pb(II) ions from aqueous solutions by waste biomass from biotrickling filters: kinetics, isotherms, and thermodynamics. J Environ Eng. https://doi.org/10.1061/(ASCE)EE.1943-7870.0000956

Davis ML, Comwell DA (1991) Introduction to environmental engineering, 2nd edn. McGraw-Hill, New York

Faghihian H, Marageh MG, Kazemian H (1999) The use of clinoptilolite and its sodium form for removal of radioactive cesium, and strontium from nuclear wastewater and Pb^{2+}, Ni^{2+}, Cd^{2+}, Ba^{2+} from municipal wastewater. Appl Radiat Isot 50:655–660

Fergusson JE (1990) The heavy elements: chemistry, environmental impact and health effects. Pergamon Press, Oxford

Gan W, Shang X, Li XH, Zhang J, Fu X (2019) Achieving high adsorption capacity and ultrafast removal of methylene blue and Pb^{2+} by graphene-like TiO2@C. Colloids Surf A 561:218–225

Gritlin RD (1988) Principles of hazardous materials management. Lewis Publishers, Ann Arbor

Gupta VK, Srivastava SK, Mohan D, Sharma S (1997) Design parameters for fixed bed reactors of activated carbon developed from fertilizer waste for the removal of some heavy metal ions. Waste Manag 17:517–522

Hamidzadeh S, Torabbeigi M, Shahtaheri SJ (2015) Removal of crystal violet from water by magnetically modified activated carbon and nanomagnetic iron oxide. J Environ Health Sci Eng. https://doi.org/10.1186/s40201-015-0156-4

Heraldy E, Lestari WW, Permatasari D, Arimurti DD (2018) Biosorbent from tomato waste and apple juice residue for lead removal. J Environ Chem Eng 6:1201–1208

Hewitt CN, Metcalfe PJ, Street RA (1991) Method for the sampling and removal of ionic alkyl-lead compounds from aqueous solution using ion-exchange media. Water Res 25:91–94

Huang Y, Yang C, Sun Z, Zeng G, He H (2015) Removal of cadmium and lead from aqueous solutions using nitrilotriacetic acid anhydride modified ligno-cellulosic material. RSC Adv 5:11475–11484

Huang Y, Zeng X, Guo L, Lan J, Zhang L, Cao D (2018) Heavy metal ion removal of wastewater by zeolite-imidazolate frameworks. Sep Purif Technol 194:462–469

Jiang SD, Yao QZ, Zhou GT, Fu SQ (2012) Fabrication of hydroxyapatite hierarchical hollow microspheres and potential application in water treatment. J Phys Chem C 116:4484–4492

Khazaei M, Nasseri S, Ganjali MR, Khoobi M, Nabizadeh RN, Gholibegloo E, Nazmara S (2018) Selective removal of lead ions from aqueous solutions using 1,8-dihydroxyanthraquinone (DHAQ) functionalized graphene oxide; isotherm, kinetic and thermodynamic studies. RSC Adv 8:5685–5694

Kold S, Rahbek O, Vestermark M, Overgaard S, Soballe K (2006) Bone compaction enhances fixation of weight-bearing hydroxyapatite-coated implants. J Arthroplasty 21:263–270

Kumar GS, Girija EK (2013) Flower-like hydroxyapatite nanostructure obtained from eggshell: a candidate for biomedical applications. Ceram Int 39:8293–8299

Laumakis MT, Martin PJ, Pamucku S, Owens K (1995) Proceeding of the international conference on hazard waste management, New York, ASCE, pp 528–535

Li Y, Bastakoti BP, Imura M, Hwang SM, Sun Z, Kim JH, Dou SX, Yamauchi Y (2014) Synthesis of mesoporous TiO_2/SiO_2 hybrid films as an efficient photocatalyst by polymeric micelle assembly. Chem A Eur J 20:6027–6032

Li S, Zeng Z, Xue W (2018a) Adsorption of lead ion from aqueous solution by modified walnut shell: kinetics and thermodynamics. Environ Technol 1:1. https://doi.org/10.1080/09593330.2018.1430172

Li Z, Tang X, Liu K, Huang J, Peng Q, Ao M, Huang Z (2018b) Fabrication of novel sandwich nanocomposite as an efficient and regenerable adsorbent for methylene blue and Pb(II) ion removal. J Environ Manag 218:363–373

Lu F, Astruc D (2018) Nanomatherials for removal of toxic elements from water. Coord Chem Rev 356:147–164

Mager EM, Brix KV, Gerdes RM, Ryan AC, Grosell M (2011) Effects of water chemistry on the chronic toxicity of lead to the cladoceran, *Ceriodaphnia dubia*. Ecotoxicol Environ Saf 74:238–243

Malgras V, Tominaka S, Ryan JW, Henzie J, Takei T, Ohara K, Yamauchi Y (2016) Observation of quantum confinement in monodisperse methylammonium lead halide perovskite nanocrystals embedded in mesoporous silica. J Am Chem Soc 138:13874–13881

Malgras V, Henzie J, Takei T, Yamauchi Y (2018) Stable blue luminescent $CsPbBr_3$ perovskite nanocrystals confined in mesoporous thin films. Angew Chem Int Ed 57:8881–8885

Pansini M, Collella C (1990) Dynamic data on lead uptake from water by chabazite. Desalination 78:287–295

Pon-On W, Charoenphandhu N, Tang IM, Jongwattanapisan P, Krishnamra N, Hoonsawat R (2011) Encapsulation of magnetic $CoFe_2O_4$ in SiO_2 nanocomposites using hydroxyapatite as templates: a drug delivery system. Mater Chem Phys 131:485–494

Qi C, Zhu YJ, Lu BQ, Zhao XY, Zhao J, Chen F (2012) Hydroxyapatite nanosheet-assembled porous hollow microspheres: DNA-templated hydrothermal synthesis, drug delivery and protein adsorption. J Mater Chem 22:22642–22650

Reed BE, Arunachalam S, Thomas B (1994) Removal of lead and cadmium from aqueous streams using granular activated carbon columns. Environ Prog 13:60–64

Saini J, Garg VK, Gupta RK (2018) Green synthesized SiO_2@OPW nanocomposites for enhanced lead(II) removal from water. Arab J Chem 1:1. https://doi.org/10.1016/j.arabjc.2018.06.003

Sangeetha K, Vidhya G, Vasugi G, Girija EK (2018) Lead and cadmium removal from single and binary metal ion solution by novel hydroxyapatite/alginate/gelatin nanocomposites. J Environ Chem Eng 6:1118–1126

Srivastav RK, Gupta SK, Nigam KDP, Vasudevan P (1993) Use of aquatic plants for the removal of heavy metals from waste waters. Int J Environ Stud 45:43–50

Tan H, Li Y, Jiang X, Tang J, Wang Z, Qian H, Mei P, Malgras V, Bando Y, Yamauchi Y (2017) Perfectly ordered mesoporous iron-nitrogen doped carbon as highly efficient catalyst for oxygen reduction reaction in both alkaline and acidic electrolytes. Nano Energy 36:286–294

Tong S, Deng H, Wang L, Huang T, Liu S, Wang J (2018) Multi-functional nanohybrid of ultrathin molybdenum disulfide nanosheets decorated with cerium oxide nanoparticles for preferential uptake of lead(II) ions. Chem Eng J 335:22–31

Wang KW, Zhu YJ, Chen F, Cheng GF, Huang YH (2011) Microwave-assisted synthesis of hydroxyapatite hollow microspheres in aqueous solution. Mater Lett 65:2361–2363

Wu M, Liu H, Yang C (2019) Effects of pretreatment methods of wheat straw on adsorption of Cd(II) from waterlogged paddy soil. Int J Environ Res Public Health 16:205. https://doi.org/10.3390/ijerph16020205

Zhang C, Li C, Huang S, Hou Z, Cheng Z, Yang P, Peng C, Lin J (2010) Self-activated luminescent and mesoporous strontium hydroxyapatite nanorods for drug delivery. Biomaterials 31:3374–3383

Zhang X, Lin Q, Luo S, Ruan K, Peng K (2018) Preparation of novel oxidized mesoporous carbon with excellentadsorption performance for removal of malachite green and lead ion. Appl Surf Sci 442:322–331

Zhang F, Tang X, Huang Y, Keller AA, Lan J (2019) Competitive removal of Pb^{2+} and malachite green from water by magnetic phosphate nanocomposites. Water Res 150:442–445. https://doi.org/10.1016/j.watres.2018.11.057